HIGH POWER LASER
SCIENCE AND ENGINEERING

RESEARCH ARTICLE

High-energy, hundred-picosecond pulsed 266 nm mid-ultraviolet generation by a barium borate crystal

Ning Wen [1,3,5,†], Nan Wang[2,†], Nan Zong[1,3,4], Xue-Chun Lin[2], Hong-Wei Gao[1,3,4], Yong Bo[1,3,4],
Qin-Jun Peng[1,3,4], Da-Fu Cui[1,3,4], and Zu-Yan Xu[1,3,4]

[1] *Key Laboratory of Functional Crystal and Laser Technology, Technical Institute of Physics and Chemistry, Chinese Academy of Sciences, Beijing, China*

[2] *Laboratory of All-Solid-State Light Source, Institute of Semiconductors, Chinese Academy of Sciences, Beijing, China*

[3] *Key Laboratory of Solid-State Laser, Technical Institute of Physics and Chemistry, Chinese Academy of Sciences, Beijing, China*

[4] *Institute of Optical Physics and Engineering Technology, Qilu Zhongke, Jinan, China*

[5] *University of Chinese Academy of Sciences, Beijing, China*

Abstract

We present a high-energy, hundred-picosecond (ps) pulsed mid-ultraviolet solid-state laser at 266 nm by a direct second harmonic generation (SHG) in a barium borate (BaB_2O_4, BBO) nonlinear crystal. The green pump source is a 710 mJ, 330 ps pulsed laser at a wavelength of 532 nm with a repetition rate of 1 Hz. Under a green pump energy of 710 mJ, a maximum output energy of 253.3 mJ at 266 nm is achieved with 250 ps pulse duration resulting in a peak power of more than 1 GW, corresponding to an SHG conversion efficiency of 35.7% from 532 to 266 nm. The experimental data were well consistent with the theoretical prediction. To the best of our knowledge, this laser exhibits both the highest output energy and highest peak power ever achieved in a hundred-ps/ps regime at 266 nm for BBO-SHG.

Keywords: all-solid-state laser; hundred-picosecond pulse; mid-ultraviolet; high-energy laser

1. Introduction

Mid-ultraviolet (mid-UV, $\lambda = 250$–300 nm) radiation[1] with high photon energy, high pulse energy, high peak power and short pulse duration has attracted a great deal of attention in micromachining[2], fluorescence research[3], spectral analysis[4–6] and other applications. Compared with traditional excimer lasers[7], all-solid-state mid-UV lasers based on frequency conversion[8] have many advantages in applications, such as compactness, high efficiency, long lifetime, high stability and low cost of system maintenance[9]. With the rapid development of diverse near-infrared fundamental frequency laser sources and high-quality nonlinear optical (NLO) crystals, cascade second harmonic generation (SHG) has been extensively used to acquire mid-UV lasers mostly.

In the past years, high-energy and high-peak-power all-solid-state mid-UV laser sources with pulse durations

from nanoseconds (ns) to femtoseconds (fs) have been reported[10–13]. In the ns regime, a pulse energy of 500 mJ at 266 nm was obtained by using a $CsLiB_6O_{10}$ (CLBO) crystal from a 532 nm laser at 10 Hz with pulse width of approximately 7 ns[10]. Unfortunately, due to the high hygroscopicity of the CLBO crystal, it required special precautions and had to work at 150°C, which is inconvenient to use. Besides, its pulse duration was wide in the ns regime, so the thermal effect would have a negative influence on fine processing[14]. In the hundred-ps/ps regime, a representative high-energy mid-UV laser at 257.7 nm was demonstrated with a 2.74 mJ pulse energy and a 4.2 ps pulse duration using a barium borate (BaB_2O_4, BBO) crystal for green-to-UV conversion. The short pulse duration and high pulse energy make the laser have high peak power of 0.56 GW[11]. BBO crystal is a commonly available mid-UV/UV NLO crystal due to its large nonlinear coefficient ($d_{eff} = 1.75$ pm/V), moderate birefringence, better temperature stability and non-hygroscopic performance with protected coatings, even if it exhibits a spatial walk-off angle. Recently, another hundred-ps (270 ps), high-energy (133 mJ) mid-UV laser at 266 nm with peak power of 0.49 GW by sum-frequency mixing from 1064 and 355 nm in lithium triborate (LBO) crystals was

Correspondence to: Nan Zong, Technical Institute of Physics and Chemistry, Chinese Academy of Sciences, Beijing 100190, China. Email: zongnan@mail.ipc.ac.cn. Xue-Chun Lin, Institute of Semiconductors, Chinese Academy of Sciences, Beijing 100083, China. Email: xclin@semi.ac.cn.

[†] These authors contributed equally to this work.

1

realized[12], which involved three LBO crystals from 1064 to 266 nm lasers. In laser processing, hundred-ps lasers bring a smaller heat affected zone than ns lasers, and the machining accuracy can also meet numerous application requirements. In addition, fewer fs mid-UV sources have been reported. For instance, 665 fs, 2.0 mJ, 258 nm mid-UV pulses were generated by BBO-SHG with an SHG conversion efficiency of approximately 18.5% from 515.4 to 258 nm. The corresponding peak power of the mid-UV pulse was up to 3 GW[13]. Ultrashort fs lasers have complex technical requirements and the single pulse energy is limited at several mJ levels, which may reduce the working efficiency. To achieve efficient and precise material processing, it is expected to develop the higher energy, higher peak-power hundred-ps mid-UV lasers.

In this paper, we demonstrate a compact, simple, hundred-ps and high-energy mid-UV laser at 266 nm. The system is based on direct SHG of a high-energy hundred-ps green laser in BBO crystal. The fundamental green laser at 532 nm delivered a maximum pulse energy of 710 mJ with a pulse width of 330 ps at 1 Hz. With careful optimization of the length of BBO crystal based on a hundred-ps SHG numerical model with the two-photon absorption (TPA) effect, a record-high pulse energy of 253.3 mJ and peak power of 1 GW at 266 nm were obtained with a pulse width of approximately 250 ps, corresponding to an SHG conversion efficiency of 35.7%. As far as we know, this is the highest pulse energy and highest peak power at 266 nm for hundred-ps/ps BBO-SHG.

2. Experimental setup

The configuration of the experimental setup for SHG from 532 to 266 nm using BBO crystal is depicted in Figure 1. First, a homemade green 532 nm pump source was produced by LBO-SHG from a Nd:yttrium aluminum garnet (YAG) master oscillator power amplifier (MOPA) laser at 1064 nm[12]. The green laser system operated at 1 Hz with maximum radiation energy of 710 mJ at 330 ps pulse duration. It had an approximately flat-topped beam intensity

profile. In order to prevent damage to the optical components from the high-energy pulse, a beam shaping system was employed to collimate the fundamental green beam to a large radius of 10 mm (D4σ). Consequently, a BBO crystal with an ultra-large cross-section of 21 mm × 21 mm was chosen, cut at $\theta = 47.7°$ and $\varphi = 0°$ for type-I phase matching (o+o→e). All crystal surfaces have protective coatings against moisture damage. After passing through the BBO crystal, the residual 532 nm pump beam was separated from the generated mid-UV pulses using a dichroic mirror (DM) coated with high-reflection (HR) at 266 nm and antireflection (AR) at 532 nm. Considering that TPA around 266 nm inside BBO crystal may limit severely the generation of high pulse energy[13], it is very important to study carefully the characteristics of BBO crystal under a high pulse energy mid-UV laser.

3. Long picosecond second harmonic generation numerical model with two-photon absorption

In order to obtain high-energy mid-UV generation, the optimal nonlinear crystal length should be designed. First, an SHG theoretical model based on coupled-wave equations describing propagation of the long ps pulses was introduced. The linear absorption, pump depletion, beam spatial birefringent walk-off and TPA effect were taken into account in the numerical model. Then, the SHG equations can be described by the following expressions[15,16]:

$$\frac{\partial A_1(x,y,z,t)}{\partial z} = -\frac{\gamma_1}{2}A_1(x,y,z,t) + P_1(x,y,z,t),$$

$$\frac{\partial A_2(x,y,z,t)}{\partial z} = -\tan\rho\frac{\partial A_2(x,y,z,t)}{\partial x}$$
$$-\frac{1}{2}\left(\gamma_2 + \beta|A_2|^2\right)A_2(x,y,z,t) + P_2(x,y,z,t),$$
$$(1)$$

where A_1 and A_2 are the spatial and temporal complex amplitudes of the fundamental frequency wave and the SH wave, respectively, ρ is the walk-off angle, γ_1 and γ_2 are linear absorption coefficients at the fundamental wave and SH wave, respectively, and β is the TPA coefficient of the
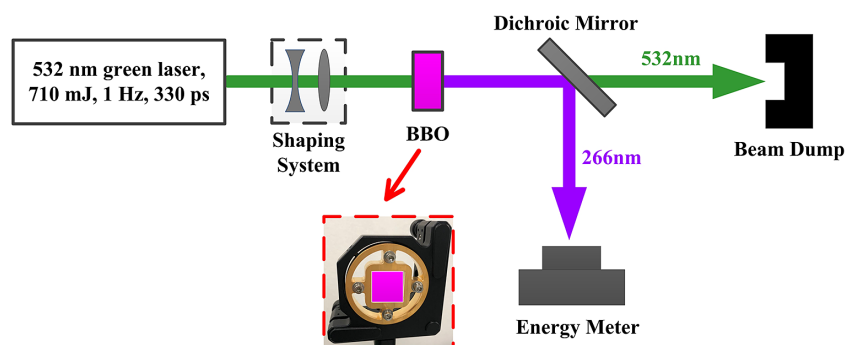
Figure 1. Schematic diagram of the BBO-SHG setup. Inset: photograph of a BBO crystal with cross-section of 21 mm × 21 mm.

SH beam. Here, P_1 and P_2 are nonlinear interaction terms, which are given by the following:

$$P_1(x,y,z,t) = j\sigma_1 A_2 A_1^* \exp(i\Delta kz),$$
$$P_2(x,y,z,t) = j\sigma_2 A_1^2 \exp(-i\Delta kz), \quad (2)$$

where $\sigma_i = \omega_1 d_{\text{eff}}/n_i c$ $(i = 1, 2)$ is the second-order nonlinear coupling coefficient, $\Delta k = 2k_1 - k_2$ is the wave vector mismatch, ω_1 is the angle frequency of the fundamental wavelength, d_{eff} is the effective nonlinear coefficient of the BBO crystal, n_1 and n_2 are the refractive indices of the BBO crystal at the pump wavelength and SH wavelength, respectively and c is the speed of light in vacuum. By the Fourier transform and fourth-order Runge–Kutta method in powerful MATLAB software, the above equations can be solved numerically. The theoretical model is similar to that of SNLO free software[17], while our numerical calculation can not only run in batches but also has more accurate results with finer grids through the crystal in the z direction. Then, we can obtain much useful information about mid-UV SH output from the BBO crystal, such as the optimal length of the NLO crystal, output energy, optical conversion efficiency and temporal profile.

4. Results and discussion

Based on the above model, the optimal length of BBO crystal can be determined. Figure 2 presents the calculated SH output energy versus crystal length at given input energy of 700 mJ with spot radius of 10 mm. The parameters used in the theoretical simulation are as follows: $\beta_2 = 0.9$ cm/GW [18], $\rho = 85.30$ mrad, $d_{\text{eff}} = 1.75$ pm/V[19,20], $\gamma_1 = 0.01$ cm^{-1} and $\gamma_2 = 0.17$ cm^{-1}[20]. In Figure 2, it can be observed that the mid-UV output energy increases progressively up to a maximum value of approximately 268 mJ around the crystal length of approximately 3 mm, corresponding to the optical-to-optical conversion efficiency of 38%. Afterwards, the saturation effect occurs for a longer crystal due to the thermal effects caused by TPA[13]. Therefore, we employed a 3-mm-long BBO crystal with aperture of 21 mm × 21 mm as the SHG crystal in the following experiment.

The experimental and the simulated mid-UV output energies at 266 nm as a function of the input pump energy are depicted in Figure 3. The black filled circles describe the experimental data measured by an energy meter (Coherent, J-50MB-YAG). As seen from Figure 3, the SH mid-UV pulse energy grows monotonously with the increasing input pump energy. Maximum output energy as high as 253.3 mJ was achieved under a pump energy of 710 mJ, which represents an SHG conversion efficiency of 35.7%. As far as we know, this mid-UV pulse energy is almost two times higher than the previous best result reported in Ref. [12]. Similarly, the
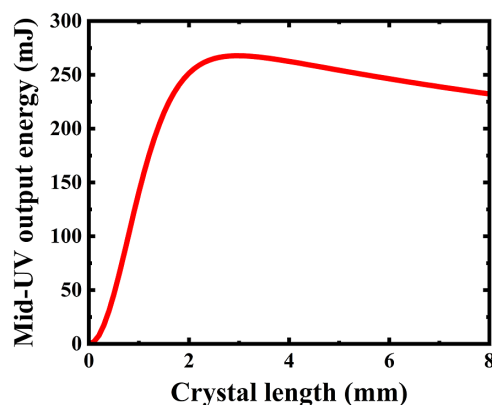

Figure 2. Calculated mid-UV output energy at 266 nm versus BBO crystal length under a 700 mJ, 532 nm pump with beam radius of 10 mm.
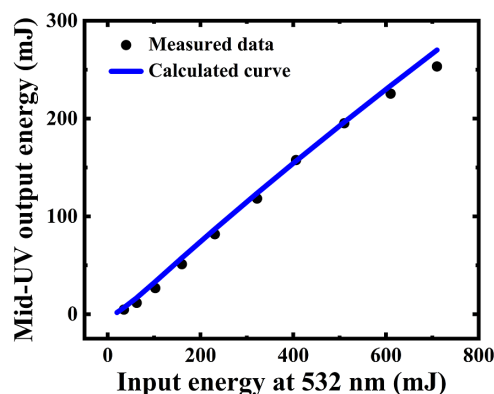

Figure 3. Mid-UV 266 nm output pulse energy versus input green pump energy at 532 nm.

simulated output results with TPA as a function of the pump energy are shown in Figure 3, indicated with a blue line. Obviously, the measured data in black dots are in close agreement with the calculated curve with TPA. Therefore, we think our long ps SHG numerical model with TPA is credible. In addition, no damage was found in the BBO crystal during the experiment.

The temporal behavior of the fundamental pulse at 532 nm was monitored by a photo-detector (Thorlabs, DET025A, rise time 150 ps) connected to a 2 GHz bandwidth digital oscilloscope (Tektronix, MSO 5204B). The typical oscilloscope trace of a single pulse profile is displayed in the Figure 4(a) at the maximum fundamental energy, suggesting the pulse duration of 332.7 ps. Owing to the lack of an appropriate photo-detector for the hundred-ps mid-UV region in our lab, we simulated the pulse width of 266 nm beam based on the above SHG numerical model. Figure 4(b) shows the temporal profile of the 266 nm radiation calculated at the full output energy by assuming the input 532 nm pulse with a Gaussian temporal profile. The estimated pulse width of 266 nm pulse was about 250 ps (full width at half maximum, FWHM), which is shorter than the incident pump pulse by a factor of $\sqrt{2}$ as the typical SHG process of a
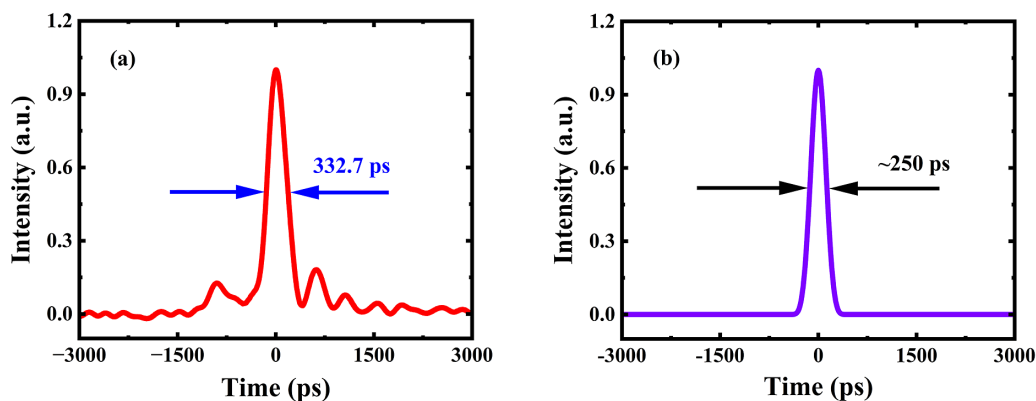
Figure 4. (a) Measured 532 nm and (b) simulated 266 nm pulse temporal profiles.
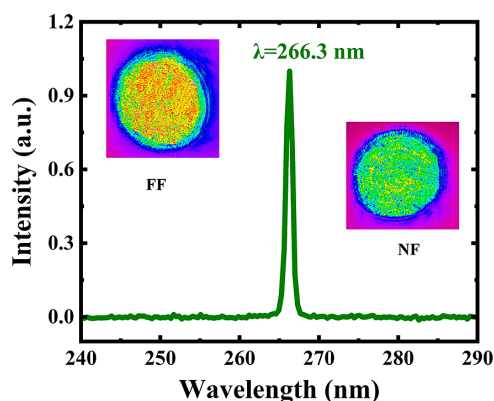

Figure 5. Spectrum of mid-UV radiation measured by a spectrometer. Inset: far-field (FF) and near-field (NF) 2D beam spatial profiles of the 266 nm mid-UV output.

Gaussian beam is due to the temporal gain narrowing effect. The rule of $\sqrt{2}$ in the SH process is approximately valid in our hundred-ps result due to a tiny group velocity delay[21]. The corresponding peak power of mid-UV pulse energy is estimated to be approximately 1 GW.

The spectrum of the generated mid-UV radiation was monitored by an optical spectrum analyzer (Avantes, AvaSpec-3648, 1.4 nm resolution) at the maximum output energy. The output mid-UV wavelength was located at 266.3 nm with the FWHM linewidth of approximately 0.6 nm, as shown in Figure 5. The inset in Figure 5 illustrates the far-field (FF) and near-field (NF) 2D beam spatial profiles of the 266 nm output, recorded using a charge-coupled device (CCD) camera (Spiricon, L11059). It can be observed in the inset of Figure 5 that the mid-UV spot is close to a round top-hat shape.

5. Conclusion

In conclusion, we have demonstrated high pulse energy, hundred-ps mid-UV radiation by SHG from a green 532 nm laser in a BBO crystal. A record-high pulse energy of 253.3 mJ at 266 nm with a repetition rate of 1 Hz was obtained when the input pulse energy at 532 nm was 710 mJ, corresponding to the SHG conversion efficiency of 35.7%. The experimental data are in reasonable agreement with the results of our theoretical simulation with the TPA. Meanwhile, the pulse duration of the mid-UV 266 nm laser was estimated by the SHG numerical model to be 250 ps and the corresponding peak power was up to 1 GW. To the best of our knowledge, these results represent the highest mid-UV pulse energy and the highest peak power at 266 nm in the hundred-ps/ps regime by BBO-SHG. This compact, simple, high-energy, high-peak-power hundred-ps mid-UV laser source provides a powerful tool in industrial and scientific applications.

References

1. R. Biswal, P. K. Agrawal, S. K. Dixit, and S. V. Nakhe, Appl. Opt. **54**, 9613 (2015).
2. N. Hodgson, A. Held, and A. Krueger, Proc. SPIE **4977**, 281 (2003).
3. O. M. Kirkby, M. Sala, G. Balerdi, R. de Nalda, L. Banares, S. Guerin, and H. H. Fielding, Phys. Chem. Chem. Phys. **17**, 16270 (2015).
4. C. A. Dailey, N. Garnier, S. S. Rubakhin, and J. V. Sweedler, Anal. Bioanal. Chem. **405**, 2451 (2013).
5. R. L. Hsiao, Y. C. Chen, M. Y. Huang, C. Y. Chen, Y. W. Lin, and C. Y. Wu, Sci. Rep. **11**, 13932 (2021).
6. A. Steube, T. Schenk, A. Tretyakov, and H. P. Saluz, Nat. Commun. **8**, 1303 (2017).
7. U. Rebhan and D. Basting, Bet. Bunsenges. Phys. Chem. **97**, 1504 (1993).

8. H. Xuan, H. Igarashi, S. Ito, C. Qu, Z. Zhao, and Y. Kobayashi, Appl. Sci. **8**, 233 (2018).

9. Z. Fang, Z. Y. Hou, F. Yang, L. J. Liu, X. Y. Wang, Z. Y. Xu, and C. T. Chen, Opt. Express **25**, 26500 (2017).

10. Y. Mori, Y. K. Yap, M. Inagaki, S. Nakajima, A. Taguchi, W. L. Zhou and T. Sasaki, Adv. Solid-State Lasers **1**, 341 (1996).

11. C. L. Chang, P. Krogen, H. Liang, G. J. Stein, J. Moses, C. J. Lai, J. P. Siqueira, L. E. Zapata, F. X. Kartner, and K. H. Hong, Opt. Lett. **40**, 665 (2015).

12. N. Wang, J. Zhang, H. Yu, X. Lin, and G. Yang, Opt. Express **30**, 5700 (2022).

13. K. Liu, H. Li, S. Qu, H. Liang, Q. J. Wang, and Y. Zhang, Opt. Express **28**, 18360 (2020).

14. B. N. Chicbkov, C. Momma, S. Nolte, F. von Alvensleben, and A. Tiinnermann, Appl. Phys. A **63**, 109 (1996).

15. F. Yang, Z. Wang, Y. Zhou, F. Li, J. Xu, Y. Xu, X. Cheng, Y. Lu, Y. Bo, Q. Peng, D. Cui, X. Zhang, X. Wang, Y. Zhu, and Z. Xu, Appl. Phys. B **96**, 415 (2009).

16. R. W. Boyd, *Nonlinear Optics*, Third Edition (Academic, New York, 2003), p. 368.

17. SNLO nonlinear optics code available from A. V. Smith, AS-Photonics, Albuquerque, NM. http://www.as-photonics.com/SNLO.

18. R. DeSalvo, A. A. Said, D. J. Hagan, E. W. V. Stryland, and M. Sheik-Bahae, IEEE J. Quantum Electron. **32**, 1324 (1996).

19. J. Sakuma, Y. Asakawa, and M. Obara, Opt. Lett. **29**, 92 (2004).

20. D. N. Nikogosyan, *Nonlinear Optical Crystals: A Complete Survey* (Springer, New York, NY, 2005), p. 6.

21. W. Kaiser, Top. Appl. Phys. **60**, 38 (1988).